American Mineralogist, Volume 79, pages 24–30, 1994

Ferroelastic phase transition along the join $CaAl_2Si_2O_8$-$SrAl_2Si_2O_8$

Martin D. McGuinn
Department of Geology, University of Manchester, Manchester M13 9PL, England
Simon A. T. Redfern
Department of Geology and Department of Chemistry, University of Manchester, Manchester M13 9PL, England

Abstract

A representative series of feldspars of composition $Ca_{1-x}Sr_xAl_2Si_2O_8$ has been synthesized. The cell parameters have been measured as a function of composition, and a continuous ferroelastic transition from monoclinic to triclinic observed at $Ca_{0.09}Sr_{0.91}Al_2Si_2O_8$ on increasing Ca content. Ferroelastic and coelastic strains arise in the triclinic phase and indicate that the transition may be modeled in terms of coupled order parameters (primary ferroelastic and secondary coelastic) within the framework of Landau theory. The primary order parameter suggests behavior according to a second-order model.

Introduction

All feldspar structures may be derived from the holosymmetric $C2/m$ form, yet few actually show such disordered monoclinic structure. In particular, anorthite, $P\bar{1}$ at room temperature, deviates furthest from the aristotype. Within a hierarchy of possible feldspar structures, it is possible to trace transition pathways from the $C2/m$ aristotype to the $P\bar{1}$ anorthite structure (Fig. 1). The interactions between transitions on this pathway have been a recent focus of attention (Carpenter, 1992), since it is clear that the thermodynamic properties of plagioclase can only be fully described by considering all such interactions. The $I\bar{1}$-$P\bar{1}$ transition, closest to room temperature (and in fact the only transition in Fig. 1 to occur below the melting point in anorthite), has been well documented, most recently by Van Tendeloo et al. (1989), Salje (1987), and Redfern and Salje (1992). However, the additional phase transitions that the anorthite structure would undergo in the absence of melting have, until recently, been largely ignored because of the obvious difficulties inherent in their direct observation. These transitions do, nonetheless, still affect the subsolidus behavior of anorthite. For example, by extrapolation of their calorimetric data on the $I\bar{1}$-$C\bar{1}$ Al-Si ordering transition in intermediate plagioclase feldspars, Carpenter et al. (1985) first estimated a transition temperature for the same transition in anorthite well above the melting point; the effects of this transition have been taken into account by Salje (1987) in his thermodynamic treatment of the $I\bar{1}$-$P\bar{1}$ transition. The equilibrium thermodynamic properties of Al-Si ordering in anorthite have been thoroughly explored in a further investigation by Carpenter (1992), and the $C\bar{1}$-$I\bar{1}$ transition appears to be first order, with a transition temperature, $T_{tr} \approx 2595$ K.

At still higher temperatures, a further displacive framework collapse is expected with the symmetry change $C\bar{1}$-$C2/m$, analogous to the analbite-monalbite transition. This proposed framework collapse is intriguing in a number of ways; not only could it have a bearing on the lower temperature $C\bar{1}$-$I\bar{1}$ and $I\bar{1}$-$P\bar{1}$ transitions, but it would also be the only true ferroelastic distortion in this family of structural transitions (with Aizu group $2/mF\bar{1}$: Aizu, 1970). Evidence for the nature of the $C2/m$-$C\bar{1}$ transition in anorthite is scarce: Carpenter (1992) points out that high-temperature measurements of cos α cannot conclusively define the transition character but would place it at 5220 K if it is second order or at 3170 K if it is tricritical. A linear extrapolation of the phase boundary in Na-rich plagioclase as a function of composition (from the data of Carpenter, 1988, and Kroll and Bambauer, 1988) would suggest a $C2/m$-$C\bar{1}$ transition at 3320 K for pure anorthite. The uncertainty in both the extrapolation to high temperature for anorthite and the extrapolation to high Ca content for the plagioclase data is very great. This study focuses on the monoclinic-triclinic distortive transition in 1:1 Al:Si feldspar, but away from the Ca end-member.

Although the monoclinic-triclinic transition in pure anorthite is effectively inaccessible by high-temperature study, it is still possible to observe the transition as a function of composition. The substitution of Ca^{2+} in the M site by a larger alkaline-earth cation such as Sr^{2+} or Ba^{2+} stabilizes the monoclinic form. Historically, the $CaAl_2Si_2O_8$ triclinic structure has been thought of as collapsed about the small Ca^{2+} sites. The larger Sr^{2+} or Ba^{2+} cations are able to hold open the structure, thereby increasing the symmetry. The exact nature of the monoclinic-triclinic collapse in $Ca_{1-x}Sr_xAl_2Si_2O_8$ is, however, uncertain. Although the M cation size must certainly have a bearing on the stability of either polymorph, the transition may still be essentially displacive, driven by the instability of the aluminosilicate framework, as in albite (Salje and Kuscholke, 1984).

The monoclinic-triclinic transition in the system

0003–004X/94/0102–0024$02.00

$Ca_{1-x}Sr_xAl_2Si_2O_8$ has been investigated as a function of composition and temperature in a number of studies (Bambauer and Nager, 1981; Bruno and Gazzoni, 1968; Sirazhiddinov et al. 1971). Nager et al. (1970) have suggested a room-temperature transition at $Ca_{0.09}Sr_{0.91}Al_2Si_2O_8$ as a function of composition. Single-crystal X-ray diffraction by Bruno and Gazzoni (1970) showed that the space group of the Sr end-member is $I2/c$ and that the c repeat is 14 Å, characteristic of a high degree of long-range Al-Si order. The transition in the series $Ca_{1-x}Sr_xAl_2Si_2O_8$ corresponds to the symmetry change $I2/c$-$I\bar{1}$. There must be a further change to $P\bar{1}$ as the Ca content increases toward anorthite. Although the $I2/c$-$I\bar{1}$ transition boundary has been pinpointed, the essential ferroelastic order parameter, the spontaneous strain, has not been measured for $Ca_{1-x}Sr_xAl_2Si_2O_8$. Furthermore, in the light of recent advances in the application of Landau theory to the problem of coupled transition phenomena in anorthite, it seems appropriate to tackle the question of the precise nature of the $I2/c$-$I\bar{1}$ transition in the $Ca_{1-x}Sr_xAl_2Si_2O_8$ series and to assess its implications for the $I\bar{1}$-$P\bar{1}$ and $I\bar{1}$-$C\bar{1}$ transitions in anorthite. Here, we have extended the scope and increased the compositional resolution of previous studies. We present the results of new spontaneous strain measurements for the $Ca_{1-x}Sr_xAl_2Si_2O_8$ feldspars, analyzing the dependence of the order parameter for the $I2/c$-$I\bar{1}$ transition on composition. Evidence for order-parameter coupling (possibly to Al-Si disordering, corresponding to a C face centered to I face centered transition) is explored, and the results are interpreted within a Landau model for the equilibrium thermodynamic behavior of anorthite and $Ca_{1-x}Sr_xAl_2Si_2O_8$ feldspars.

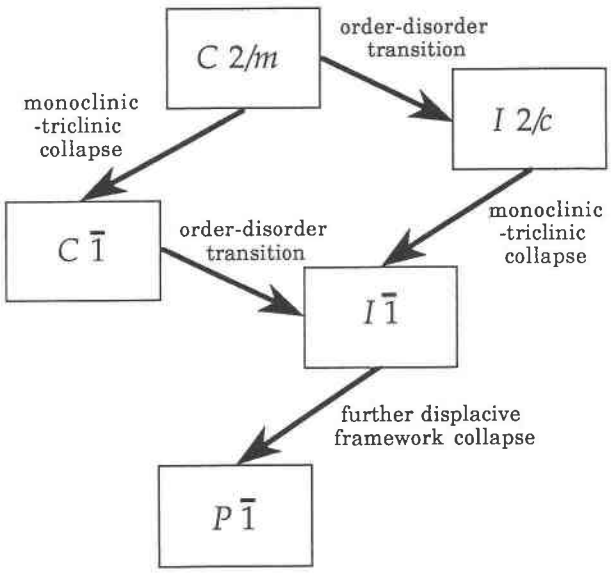

Fig. 1. Hierarchy of phase transitions in feldspar. The $I2/c$-$I\bar{1}$ transition is the only ferroelastic transition possible in 2:2 Al:Si feldspar.

Experimental methods

Synthesis

A series of samples was synthesized along the $Ca_{1-x}Sr_xAl_2Si_2O_8$ join, with values of x = 1.00, 0.95, 0.90, 0.85, 0.80, 0.75, 0.70, 0.65, 0.60, 0.50, 0.40, 0.30, 0.20, 0.10, 0.00. The synthesis technique broadly follows that described by Bambauer and Nager (1981).

Each sample was prepared by accurately weighing a stoichiometric mixture of the component oxides Al_2O_3, SiO_2, $CaCO_3$, and $SrCO_3$ (the Ca and Sr components were included in the initial mixtures as carbonates because of the extremely hygroscopic nature of their oxides) to give a total mass of $Ca_{1-x}Sr_xAl_2Si_2O_8$ of 5.0 g. The mixtures were then ground by hand in an agate mortar for 30 min to obtain a very fine mixture more suited to solid-state reaction. These mixtures were annealed at 1 atm in a Pt crucible at 1073 K for 24 h to decarbonate the $CaCO_3$. Further heating at 1573 K for 24 h followed to decarbonate the $SrCO_3$ before the mixtures were finally annealed at 1773 K for 72 h to allow the crystalline feldspar to form by a solid-state reaction. Samples were air cooled without any specific additional quench. Typically, synthesis products were slightly sintered and were disaggregated by crushing in an agate pestle and mortar. On one occasion, partial melting occurred (resulting in a fused synthesis product) when the furnace exceeded a preset temperature in error, and this sample was discarded. None of the samples used in this study showed any evidence of a glass component in the background intensities of X-ray diffraction patterns.

Although Bambauer and Nager (1981) suggested that equilibrium samples can be produced in 24 h at 1773 K, we found that a 72-h synthesis time was necessary to produce crystalline material that showed no signs of particle size broadening in X-ray diffraction patterns.

Care was taken to ensure that annealing conditions were kept consistent throughout each synthesis experiment to guarantee that the samples across the series maintained structural states as nearly identical as possible. The structural homogeneity of each sample was verified using conventional X-ray diffraction techniques. In each case the diffraction pattern corresponded to a single crystalline feldspar phase.

Each sample was analyzed by electron microprobe, and all compositions were found to be within 1 mol% of the expected value.

Determination of room-temperature lattice parameters

Room-temperature lattice parameters were obtained from high-resolution Guinier X-ray powder diffraction patterns using a Huber 620 Guinier powder diffraction camera with Cu$K\alpha_1$ radiation. National Bureau of Standards Si powder was ground and mixed with the finely ground sample to act as an internal standard, enabling zero-error and film-shrinkage corrections when the patterns were measured and indexed. The sample and standard mixture were then mounted on Mylar film using collodion as a fixing medium. Operating conditions of 40

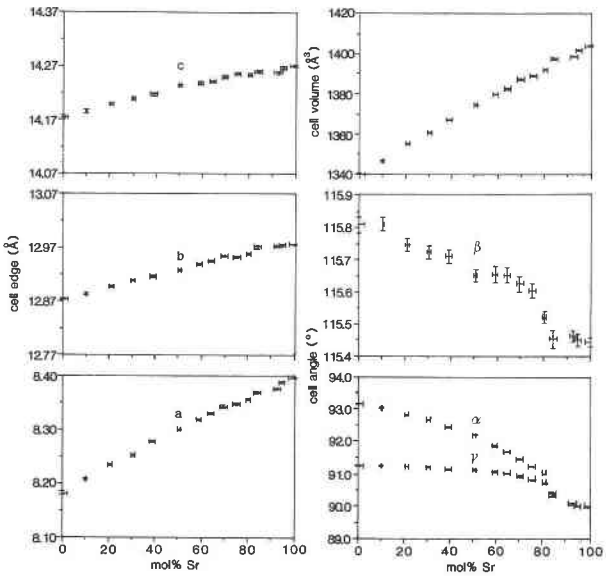

Fig. 2. Cell parameters of $Ca_{1-x}Sr_xAl_2Si_2O_8$ as a function of composition. Error bars represent $\pm\sigma$. Note the difference in scale between β and the other cell angles.

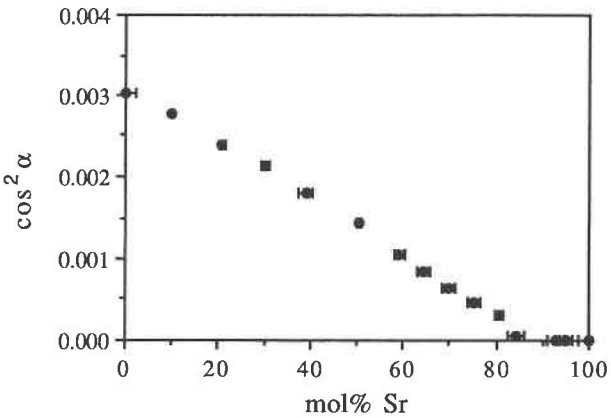

Fig. 3. $Cos^2\alpha$ for triclinic feldspar along the $Ca_{1-x}Sr_xAl_2Si_2O_8$ join, showing $\cos^2\alpha \propto |x_c - x|$, $x_c = 0.91$.

kV and 20 mA were used, and exposure times of approximately 15 h were found to be necessary because of the poor scattering power of the samples. Films were measured using a traveling video microscope system to a precision of 0.005° 2θ, with a typical error on line measurement of $\pm 0.01°$ 2θ.

The powder patterns were indexed by comparison with the anorthite pattern of Borg and Smith (1968) and by generating theoretical powder patterns for strontian anorthite based on the single-crystal data of Bruno and Gazzoni (1970), using at least 36 indexed lines in triclinic refinements. The monoclinic lines split in the triclinic samples, and split pairs commonly cross one another. Care was taken to ensure that indexing was faultless by charting the positions of split peaks as a function of composition. Lattice parameters were obtained by least-squares refinement of the powder diffraction data, with a typical error of 0.001 Å in the cell edges and 0.01° in the cell angles.

The agreement between the parameters determined for our $SrAl_2Si_2O_8$ and those of Bambauer and Nager (1981) suggests that our Sr-rich samples are relatively well ordered and correspond to space group $I2/c$ rather than $C2/m$ [as has been reported for certain nonstoichiometric strontian feldspar (Grundy and Ito, 1974)]. Any small difference in cell parameters between our samples and those of Bambauer and Nager may be due to the slightly longer annealing time that we employed. There is, however, a large discrepancy between our cell parameters and those obtained by Bruno and Gazzoni (1968), who employed a fusion synthesis technique. It is possible that their synthesis technique produced disequilibrium samples that were nonstoichiometric, although there are no analyses to confirm this. Nonetheless, they observed similar trends in their cell parameters across the solid solution, although their results suggest a more calcic room-temperature transition composition of approximately $Ca_{0.77}Sr_{0.23}Al_2Si_2O_8$.

We further explored the degree of Al-Si order in the Ca

Table 1. Unit-cell parameters of the series $Ca_{1-x}Sr_xAl_2Si_2O_8$

x	a	b	c	α	β	γ	V
1.00(2)	8.395(1)	12.977(1)	14.270(1)	90.00(0)	115.44(1)	90.00(0)	1403.8(2)
0.93(2)	8.386(1)	12.976(1)	14.267(2)	90.00(0)	115.45(1)	90.00(0)	1401.8(2)
0.91(2)	8.375(1)	12.974(2)	14.258(2)	90.08(1)	115.46(1)	90.09(1)	1398.6(2)
0.86(2)	8.368(2)	12.972(2)	14.259(2)	90.42(2)	115.45(2)	90.32(2)	1397.4(3)
0.81(1)	8.355(1)	12.959(1)	14.254(1)	91.02(1)	115.52(1)	90.73(1)	1392.0(2)
0.76(2)	8.346(2)	12.953(2)	14.255(2)	91.22(2)	115.60(2)	90.82(1)	1389.0(2)
0.72(1)	8.341(2)	12.955(2)	14.249(2)	91.44(2)	151.62(2)	90.93(1)	1387.2(3)
0.65(1)	8.329(2)	12.945(2)	14.241(2)	91.67(1)	115.65(2)	91.01(1)	1382.7(2)
0.58(2)	8.318(2)	12.939(2)	14.238(2)	91.86(2)	115.65(2)	91.07(1)	1379.7(3)
0.52(1)	8.299(1)	12.928(1)	14.233(1)	92.18(1)	115.65(1)	91.13(1)	1374.5(2)
0.41(1)	8.277(1)	12.916(1)	14.217(2)	92.43(1)	115.71(1)	91.15(1)	1367.0(2)
0.30(1)	8.252(1)	12.908(1)	14.209(2)	92.64(1)	115.72(1)	91.20(1)	1360.7(2)
0.21(1)	8.235(1)	12.898(1)	14.198(2)	92.81(1)	115.75(1)	91.22(1)	1355.2(2)
0.10(1)	8.207(1)	12.883(2)	14.185(2)	93.01(1)	115.81(1)	91.25(1)	1346.7(2)
0.00(2)	8.181(2)	12.874(2)	14.174(2)	93.15(2)	115.81(2)	91.26(1)	1340.2(2)

Note: values for a, b, and c are given in ångströms; values for α, β, and γ are given in degrees; values for V are given in cubic ångströms.

end-member sample using the method of Carpenter et al. (1990). Comparing the room-temperature cell parameters for our sample with those for the $C\bar{1}$ anorthite of Carpenter et al. (1990), which were crystallized from glass, we obtain a scalar strain due to Al-Si order of $e_{s(od)} = 0.0073$, corresponding to a value of the Al-Si order parameter, Q_{od}, for this sample of 0.85. Preliminary MAS NMR data on these samples confirm these results and furthermore suggest that the $SrAl_2Si_2O_8$ sample has $Q_{od} \geq 0.90$ (Kohn, personal communication).

Results and discussion

Cell parameters and critical transition composition

The room-temperature cell parameters of the $Ca_{1-x}Sr_xAl_2Si_2O_8$ series are shown as a function of composition in Figure 2 and Table 1.

The cell parameters reveal a structural phase transition in the series as a function of composition. Most noticeably, the α and γ cell angles deviate from 90° in the monoclinic cell of the Sr-rich members to 93.15 and 91.25°, respectively, in the triclinic Ca end-member. The increase in both angles is smooth and continuous and is the first suggestion that the transition itself is continuous. The α cell parameter shows a greater deviation from 90° than the γ cell parameter and is a more sensitive probe of the transition. The β cell angle and the cell edges appear to vary linearly with composition: both β and b display a slight change in slope with respect to composition at the transition.

The cell volume varies linearly with composition and shows no change in slope at the transition. The cell parameters suggest that the dominant symmetry-breaking process is a shearing in the (100) and (001) planes, causing the α and γ angles to deviate from 90°. The way in which a cell angle such as α deviates from 90° is a measure of the degree of triclinicity of a feldspar. Such a measure can be understood within Landau theory as an order parameter for a triclinic feldspar (Carpenter, 1988). For the series $Ca_{1-x}Sr_xAl_2Si_2O_8$, it is found that $\cos^2\alpha$ varies linearly with composition (Fig. 3) and becomes zero (the unit cell becomes monoclinic) with increasing Sr content at the composition $Ca_{0.09}Sr_{0.91}Al_2Si_2O_8$. This result is in good agreement with those of Nager et al. (1970), although the improved composition resolution of our work enables the placement of this point as the critical composition for the phase transition with greater confidence. The composition-dependent order parameter behavior below x_c is now described from spontaneous strain measurements.

Spontaneous strain and order parameter coupling

The components of the spontaneous strain tensor may be formulated in terms of the lattice parameters using a Cartesian coordinate system with R_2 parallel to the crystallographic **b** axis, R_3 parallel to the crystallographic **c*** axis, and R_1 perpendicular to both (in accordance with the Cartesian coordinate system adopted by Ryzhova, 1964).

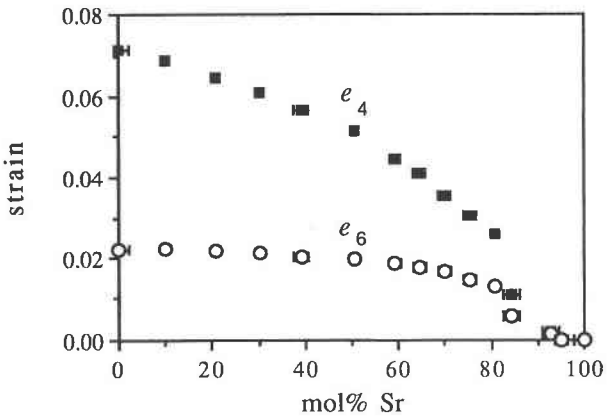

Fig. 4. Ferroelastic strain components (e_4 and e_6) as a function of composition. Note that e_4 scales differently than e_6 as a function of composition.

The transition $I\bar{1}$-$I2/c$ is associated with critical phonons at the center of the Brillouin zone (Γ point). If the transition is pure ferroelastic, these are acoustic phonons associated with the softening of the elastic constants that are symmetry-forbidden in the monoclinic phase. The order parameter for the transition behaves as the active representation, B_{1g}, in $I2/c$, and the transition induces strain components e_4 (= $2e_{23}$ and e_6 (= $2e_{12}$). These strains are related to the cell parameters (following Redfern and Salje, 1987) by

$$e_4 = \frac{c\cos\alpha}{c_o \sin\beta_o^*} + \frac{\cos\beta_o^*}{\sin\beta_o^*}(\cos\gamma) \quad (1)$$

$$e_6 = \cos\gamma. \quad (2)$$

where the subscript o refers to the paraelastic reference state and denotes the relevant parameter that might be expected, by extrapolation, in a sample of identical composition in the absence of the phase transition, i.e., if the cell had remained monoclinic.

The true ferroelastic nature of the transition, as witnessed by switching of ferroelastic domains in the low-symmetry phase, has yet to be verified. Since e_4 and e_6 are the only symmetry-required components of the spontaneous strain tensor, they will be referred to as ferroelastic strain components. The triclinic distortion of the unit cell becomes greater with increasing Ca in the solid solution, and the ferroelastic strain elements reflect directly the composition dependence of the distortive order-parameter below the $I\bar{1}$-$I2/c$ transition. These ferroelastic strain components are shown in Figure 4.

Other elements of the triclinic spontaneous strain tensor (coelastic strain components) that are not required by symmetry are, nonetheless, observed. They are given by

$$e_1(= e_{11}) = \sin\gamma - 1 \quad (3)$$

$$e_2(= e_{22}) = \frac{b}{b_o} - 1 \quad (4)$$

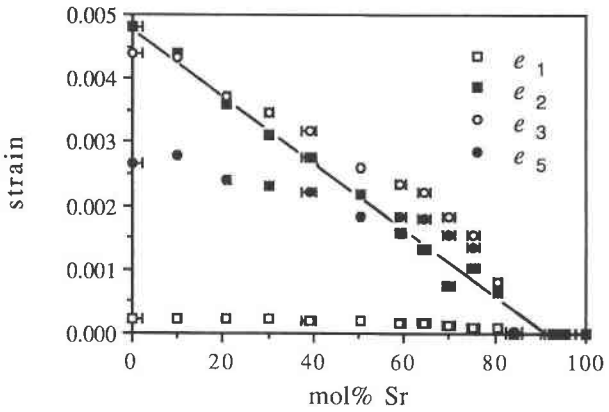

Fig. 5. Coelastic strain components (e_1, e_2, e_3, e_5) as a function of composition. The line shows a linear fit to e_2, indicating $e_2 \propto |x_c - x| \propto Q_s^2$, the secondary (coelastic) order parameter.

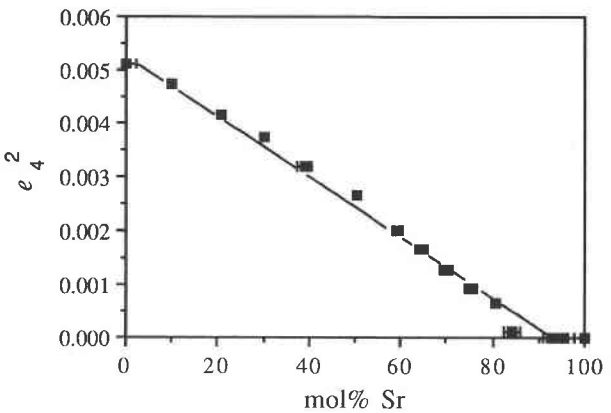

Fig. 6. Plot of e_4^2 as a function of composition. The line shows a linear fit, implying $e_4 \propto Q_o \propto |x_c - x|^{1/2}$ for the primary order parameter.

$$e_3(= e_{33}) = \frac{(\sin \alpha)(\sin \beta^*)}{\sin \beta_o^*} - 1 \quad (5)$$

$$e_5(= 2e_{13}) = \frac{(\sin \gamma)(\cos \beta_o^*)}{\sin \beta_o^*} - \frac{(\sin \alpha)(\cos \beta^*)}{\sin \beta_o^*}. \quad (6)$$

These strain components are shown in Figure 5. The coelastic strains are an order of magnitude smaller than the ferroelastic strains and are of the same order as coelastic strains reported from other feldspar examples, e.g., those arising below the $I\bar{1}$-$P\bar{1}$ transition in anorthite (Redfern and Salje, 1987). Since the coelastic strains are nonzero, the $I2/c$-$I\bar{1}$ transition in $Ca_{1-x}Sr_xAl_2Si_2O_8$ feldspars cannot be described by a single ferroelastic process but involves at least one other order parameter that induces the coelastic strains observed. The two processes arise simultaneously for members of the solid solution more calcic than $Ca_{0.09}Sr_{0.91}Al_2Si_2O_8$ and are likely to be coupled through the strains.

Landau model for the $I2/c$-$I\bar{1}$ structural phase transition

$I\bar{1}$ is a subgroup of $I2/c$, and the transition is potentially second order, since the symmetry reduction satisfies both the Landau and Lifschitz criteria. It is therefore possible to model the excess thermodynamic properties using a Landau formulation in terms of a 2-4-6 potential, with additional strain-order parameter coupling. Ignoring, for the moment, the coelastic features observed, the excess Gibbs energy would then be described by

$$\Delta G = \tfrac{1}{2}a(T - T_c)Q_o^2 + \tfrac{1}{4}bQ_o^4 + \tfrac{1}{6}cQ_o^6 + \sum_i \lambda_i Q_o e_i + \sum_{ik} C_{ik} e_i e_k \quad (7)$$

where C_{ik} are the elastic constants and λ_i are the coupling constants between the order parameter for the ferroelastic process, Q_o, and the ferroelastic components of the spontaneous strain tensor. The ferroelastic spontaneous strain transforms according to the active representation B_{1g} and couples linearly with the order parameter.

The above expression would normally be applied to temperature-dependent phase transitions. In this study, where the transition is observed as a function of solid-solution composition at constant temperature, a term may be added to the free-energy expansion to allow for composition-order parameter coupling. Salje et al. (1991) showed that the lowest coupling allowed between the molar fraction of $SrAl_2Si_2O_8$, x, and the order parameter is linear quadratic and, if one ignores higher order composition-order parameter coupling, the free energy expansion becomes

$$\Delta G = \tfrac{1}{2}a(T - T_c)Q_o^2 + \tfrac{1}{4}bQ_o^4 + \tfrac{1}{6}cQ_o^6 + \sum_i \lambda_i Q_o e_i + \sum_{ik} C_{ik} e_i e_k + \zeta x Q_o^2 \quad (8)$$

where ζ is the composition-order parameter coupling constant. In the case of a stress-free crystal, $d(\Delta G)/de_i = 0$, and hence

$$e_i = M_i(C_{ik}, \lambda_i)Q_o \quad (9)$$

where M_i are constants dependent upon the elastic constants and strain-order parameter coupling constants. Thus

$$\Delta G = \tfrac{1}{2}a\left[T - T_c + (2\lambda_i M_i + C_{ik}M_iM_k)/a + 2\frac{\zeta x}{a}\right]Q_o^2 + \tfrac{1}{4}bQ_o^4 + \tfrac{1}{6}cQ_o^6 \quad (10)$$

and so the transition temperature is renormalized by ζx in our experiments, with the renormalized critical temperature, T_c^*, given by

$$T_c^* = T_c - (2\lambda_i M_i + C_{ik}M_iM_k)/a - 2\frac{\zeta x}{a}. \quad (11)$$

The order parameter below the phase transition would be expected to follow the relation $Q_o \propto |T_c - T|^{\beta}$. However, for the purpose of this study, temperature and pres-

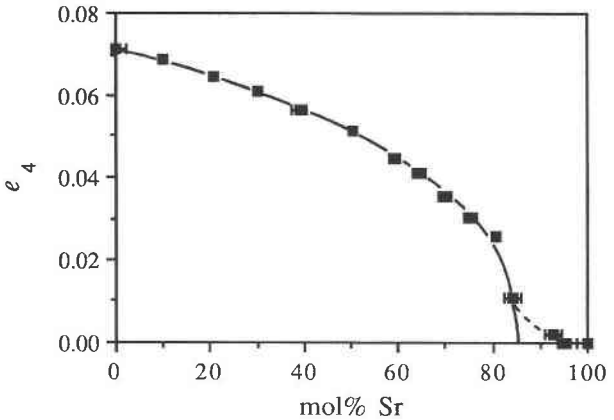

Fig. 7. Least-squares analysis of e_4 as a function of composition gives the relationship $e_4 = 0.076(0.86 - x)^{\beta}$, $\beta = 0.40$. The dotted line indicates a possible strain tail close to the critical composition for the transition.

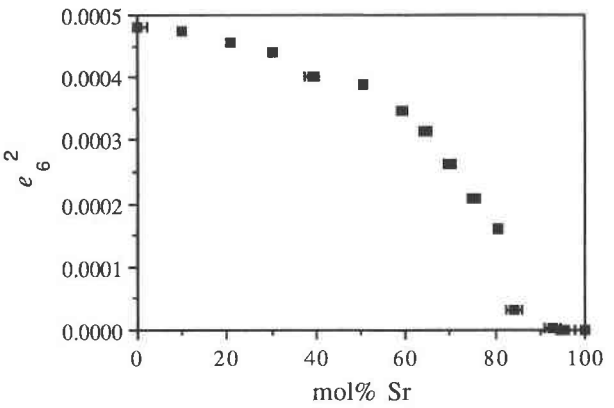

Fig. 8. Plot of e_6^2 as a function of composition. Note the nonlinear nature of the curve compared with e_4^2 as a function of composition, which highlights the difference in scaling between the two strains.

sure were kept constant while x, the molar proportion of $SrAl_2Si_2O_8$, was varied. Therefore, assuming all the coupling constants are independent of composition, we can state

$$e \propto Q_o \propto |x_c - x|^{\beta}, \qquad \text{for } x < x_c \qquad (12)$$

where x_c is the observed critical molar proportion of $SrAl_2Si_2O_8$ at which the monoclinic feldspar framework distorts.

Our measurement of e_4 and e_6 can, therefore, reveal the critical exponent for the order parameter as a function of composition. If e_4 is purely ferroelastic, Figure 6 implies $e_4^2 \propto |x_c - x|$ and $\beta = 1/2$, corresponding to a classical second-order phase transition. Closer least-squares analysis, however (Fig. 7), reveals that the composition dependence of e_4 follows the relationship $e_4 = 0.076\ (0.86 - x)^{\beta}$, $\beta = 0.40$. This would imply that the transition to monoclinic occurs at $Sr_{0.86}Ca_{0.14}Al_2Si_2O_8$, but Figure 7 also shows that there is significant triclinic strain for the $Sr_{0.90}Ca_{0.10}Al_2Si_2O_8$ sample. This result suggests that although the transition is essentially second order, it may be closer to tricritical than the first approximation of $e_4^2 \propto |x_c - x|$ implies. Alternatively the transition may be second order, but higher order coupling between Q_o and x may be operating across the composition range. If Figure 7 accurately represents the order parameter for the $I\bar{1}$-$I2/c$ transition, then the triclinic strain at $Sr_{0.09}Ca_{0.10}Al_2Si_2O_8$ could be interpreted as a fluctuation-related strain tail (dotted line), since the figure implies that T_c for this sample is just below room temperature.

We note that e_6^2 does not scale in the same way as e_4^2 (Fig. 8) and that additional strain components e_1, e_2, e_3, and e_5 arise below x_c (Figs. 4 and 5). These deviations from simple second-order behavior may be attributed to a secondary-order parameter, Q_s, which must be coupled (in lowest order) quadratically to Q_o. This could be a zone-boundary process, such as Al-Si order-disorder or another, as yet unidentified, coelastic process. It should be noted that e_4 and e_6 are allowed by symmetry to couple to both Q_o and Q_s. The remaining strain components, e_1, e_2, e_3, and e_5, may only, however, couple to the secondary-order parameter.

Carpenter (1992) has shown that the lowest order coupling between Q_o and Al-Si order in the anorthite framework is biquadratic. The lowest order coupling between such a zone-boundary process and the observed strains is $e \propto Q_s^2$. We see that in this case, e_2 is linear with respect to composition, so that if this strain is dominantly coupled by only lowest order terms, $Q_s \propto |x_c - x|^{1/2}$, and it is biquadratically coupled to Q_o. The other strain components do not scale in the same way, suggesting that higher order x-Q_s, e-Q_s, and Q_o-Q_s coupling terms are important.

These results indicate that e_4 is a good measure of Q_o, and e_2 is a good measure of Q_s in this system. Of the other strain components, e_6 reflects coupling to both Q_o and Q_s, and e_1, e_3, and e_5 reflect higher order coupling terms to Q_s. Further experimental work is required to identify the physical processes corresponding to Q_s. In particular, we are carrying out high-temperature and pressure diffraction and spectroscopic studies on these samples to characterize further the order parameter behavior and its dependence on extensive thermodynamic variables in the calcium-strontium-feldspar system.

Acknowledgments

This work was supported by the N.E.R.C. in the form of a research studentship to M.D.M., and by a grant from the Nuffield Foundation to S.A.T.R.

The authors wish to thank Brian Phillips and an unknown reviewer for their careful reviews of the manuscript and C.M.B. Henderson for his help and advice.

References cited

Aizu, K. (1970) Determination of the state parameters and formulation of the spontaneous strain for ferroelastics. Journal of the Physical Society of Japan, 28, 706–716.

Bambauer, H.-U., and Nager, H.E. (1981) Gitterkonstanten und displazive transformationen synthetischer Erdalkalifeldspäte. I. System $Ca[Al_2Si_2O_8]$-$Sr[Al_2Si_2O_8]$-$Ba[Al_2Si_2O_8]$. Neues Jahrbuch für Mineralogie Abhandlungen, 141, 225–239.

Borg, I.Y., and Smith, D.K. (1968) Calculated powder patterns. I. Five plagioclases. American Mineralogist, 53, 1709–1723.

Bruno, E., and Gazzoni, G. (1968) Feldspati sintetici della serie $Ca[Al_2Si_2O_8]$-$Sr[Al_2Si_2O_8]$. Atti della Accademia delle Scienze de Torino, 102, 881–893.

——— (1970) Single-crystal X-ray investigations on strontium feldspar. Zeitschrift für Kristallographie, 132, 327–331.

Carpenter, M.A. (1988) Thermochemistry of aluminium/silicon ordering in feldspar minerals. NATO ASI Series C, 225, 265–323.

——— (1992) Equilibrium thermodynamics of Al/Si ordering in anorthite. Physics and Chemistry of Minerals, 19, 1–24.

Carpenter, M.A., McConnell, J.D.C., and Navrotsky, A. (1985) Enthalpies of ordering in the plagioclase feldspar solid solution. Geochimica et Cosmochimica Acta, 49, 947–966.

Carpenter, M.A., Angel, R.J., and Finger, L.W. (1990) Calibration of Al/Si order variations in anorthite. Contributions to Mineralogy and Petrology, 104, 471–480.

Grundy, H.D., and Ito, J. (1974) The refinement of the crystal structure of a synthetic non-stoichiometric Sr feldspar. American Mineralogist, 59, 1319–1326.

Kroll, H., and Bambauer, H.-U. (1981) Diffusive and displacive transformation in plagioclase and ternary feldspar series. American Mineralogist, 66, 763–769.

Nager, H.E., Bambauer, H.-U., and Hoffmann, W. (1970) Polymorphie in der Mischreihe $(Ca,Sr)[Al_2Si_2O_8]$. Naturwissenschaften, 57, 86–87.

Redfern, S.A.T., and Salje, E. (1987) Thermodynamics of plagioclase. II. Temperature evolution of the spontaneous strain at the $I\bar{1}$-$P\bar{1}$ phase transition in anorthite. Physics and Chemistry of Minerals, 14, 189–195.

——— (1992) Microscopic dynamic and macroscopic thermodynamic character of the $I\bar{1}$-$P\bar{1}$ phase transition in anorthite. Physics and Chemistry of Minerals, 18, 526–533.

Ryzhova, T.V. (1964) Elastic properties of plagioclase. Akademii Nauk SSSR, Izvestiya Geofizika, Seriya 7, 1049–1051.

Salje, E. (1987) Thermodynamics of plagioclase. I. Theory of the $I\bar{1}$-$P\bar{1}$ transition in anorthite and Ca-rich plagioclases. Physics and Chemistry of Minerals, 14, 181–188.

Salje, E., and Kuscholke, B. (1984) On the structural phase transitions in alkali feldspars. Bulletin de Minéralogie, 107, 539.

Salje, E., Bismayer, U., Wruck, B., and Hensler, J. (1991) Influence of lattice imperfections on the transition temperature of structural phase transitions: The plateau effect. Phase Transitions, 35, 61–74.

Sirazhiddinov, N.A., Arifov, P.A., and Grebenshichikov, R.G. (1971) Phase diagram of strontium-calcium anorthites. Izvestiia Akademii Nauk SSSR, Neorganicheskie Materialy, 7, 1581–1583.

Van Tendeloo, G., Ghose, S., and Amelincx, S. (1989) A dynamical model for the $I\bar{1}$-$P\bar{1}$ transition in anorthite, $CaAl_2Si_2O_8$. I. Evidence from electron microscopy. Physics and Chemistry of Minerals, 16, 311–319.

Manuscript Received March 2, 1993
Manuscript accepted September 9, 1993